Temperature dependence of single-asperity friction for a diamond on diamondlike carbon interface

C. G. Dunckle,[1,a] I. B. Altfeder,[2] A. A. Voevodin,[2] J. Jones,[2] J. Krim,[3] and P. Taborek[1]
[1]*University of California, Irvine, California 92697, USA*
[2]*Materials and Manufacturing Directorate, Air Force Research Laboratory, RXBT, Wright-Patterson Air Force Base, Ohio 45433, USA*
[3]*North Carolina State University, Raleigh, North Carolina 27695, USA*

(Received 5 March 2010; accepted 26 April 2010; published online 2 June 2010)

A variable temperature, ultrahigh vacuum atomic force microscope (AFM) was used to characterize interfacial friction for a single-asperity diamond contact on a diamondlike carbon (DLC) substrate over a nominal substrate temperature range of 90 to 275 K. Calibrated friction force measurements were obtained by analyzing lateral force hysteresis loops as a function of normal force. For sufficiently large normal forces, the lateral force was proportional to the normal force, and a friction coefficient μ could be identified. μ varied approximately linearly with substrate temperature, with $\mu=0.28$ at $T=90$ K and $\mu=0.38$ at 275 K. These results are compared to other recent variable temperature AFM friction measurements and to theoretical calculations based on the Tomlinson model. This comparison is obscured by large, experimentally uncontrolled temperature differences between the tip and the substrate which inevitably exist in conventional, variable temperature AFMs. A thermal model which can be used to quantitatively estimate these temperature differences is presented. © *2010 American Institute of Physics*. [doi:10.1063/1.3436564]

I. INTRODUCTION

When an atomic force microscope (AFM) tip slides across a surface it experiences a frictional force opposite to its direction of motion. The component of the force parallel to the substrate produces a torque which causes the cantilever to twist. The degree of twist can be monitored using the appropriate combination of channels from a quadrant photodiode using the laser deflection detection method. This technique, known as friction force microscopy, has made considerable contributions to the field of single-asperity tribology.[1–3] Understanding single-asperity friction[4,5] is important for the design and operation of microscale and nanoscale electromechanical devices,[6,7] interpretation of biological lateral force imaging,[7–9] and it also provides a means for direct comparison with fundamental theories of friction.[12,13] Theoretical models of single contact friction have evolved from the early work by Tomlinson[10,14] that considered sliding of a point contact from a molecular perspective involving relaxation of metastable states. Modern versions of the theory[11–15,17,18] explicitly include the effects of thermal hopping processes using a Langevin equation. The random forces in this equation have a mean square amplitude proportional to the temperature and are constructed to obey the fluctuation dissipation theorem. Qualitatively, these theories predict that the lateral force required to move a single asperity across a surface at a constant velocity is low at high temperatures (sometimes called thermolubricity[13,19]) where thermal fluctuations facilitate hopping over barriers, and conversely, the lateral force is high at low temperatures when the fluctuations are absent.[16] Detailed predictions depend on parameters such as the surface potential corrugation and the mechanical properties of the cantilever. For some sets of parameters, the computed value of the lateral force over the temperature range considered in this paper is monotonic in temperature and varies by more than two orders of magnitude,[13] while for other parameters, the variation is nonmonotonic and varies by less than a factor of 3.[17] An alternative description of frictional interactions involves phonon-phonon coupling in the solids.[18,19] The interaction depends on the phonon density (which scales as T^4 at low temperature) and on the phonon mean free path and therefore exhibits strong temperature dependence. In contrast to the Tomlinson hopping mechanism, phononic friction tends to increase with increasing temperature, as shown in recent simulations.[20] Phononic vibration in adsorbed surface layers has been applied in recent AFM measurements of hydrogen and deuterium terminated diamond and silicon surfaces to explain experimentally observed differences in friction levels.[21]

There have been several previous experimental investigations of the temperature dependence of friction using a variety of AFM tip-surface material combinations including measurements using silicon and silicon nitride tips sliding on highly ordered pyrolytic graphite,[15,22] silicon,[23] molybdenum disulfide,[24] etc. The results show a rapid increase in the friction by more than an order of magnitude as the temperature is lowered below a characteristic temperature in the range of 100–250 K. Zhao *et al.*[22,24] have applied an Arrhenius analysis to their data and more recently looked at the effects of wear. Results using diamond-coated tips on single crystal diamond samples have revealed a more modest variation over the temperature ranges reported.[25] The original goal of this work was to extend the study of the temperature dependence of single-asperity friction to diamondlike carbon (DLC), an amorphous alloy of carbon and hydrogen. DLC is

[a]Electronic mail: cdunckle@uci.edu.

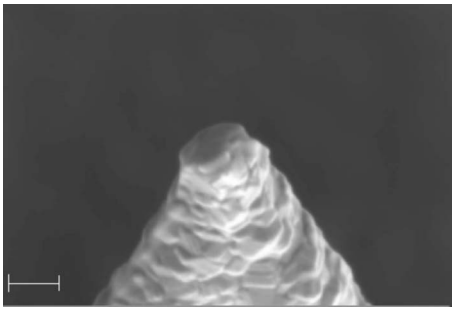

FIG. 1. Scanning electron microscope image of an unused AFM tip (NanoSensors Inc., DT-CONTR) of the same variety as the one used in this experiment. The scale bar represents 200 nm.

well suited to AFM studies because smooth, flat samples are readily available and it provides a useful comparison to previous single crystal studies. Diamondlike materials are of particular engineering interest because of their outstanding properties including chemical inertness, hardness, resistance to wear, and extremely low coefficient of friction. The room temperature macroscopic tribological behavior of hydrogenated DLC has been extensively studied[26–28] and shows that the macroscopic friction coefficient increases slightly at low temperature, but remains below 0.1 down to $T=50$ K.[29] During our data analysis it became clear that the substrate temperature could be very different from the AFM tip temperature. This indicated that our measurements and similar previous measurements may not be well suited for determining the temperature dependence of friction in single-asperity contacts. We present a detailed model of heat transfer from the AFM cantilever to the substrate which quantifies this effect. The results imply that measurements of the lateral force as a function of substrate temperature taken using a variable temperature AFM do not adequately represent the physics at the sliding contact.

II. METHODOLOGY AND RESULTS

A commercial, variable temperature UHV AFM (RHK 750) equipped with a continuous flow helium cryostat was used to generate substrate temperatures in the range of 90 to 275 K. The sample stage was connected to the cold finger by a copper braid. A LakeShore Si diode thermometer was epoxied to the side of the sample stage providing accurate temperature readings from 2 to 300 K. The silicon cantilevers obtained from NanoSensors Inc. (DT-CONTR) had 100 nm of polycrystalline diamond on the bottom surface as shown in Fig. 1 and 30 nm of reflective aluminum coating on the top surface. The nominal normal force spring constant was $K_{norm}=0.24$ N/m. A silicon wafer with a DLC coating from Morgan Advanced Ceramics, 2 μm thick and measured roughness of 0.16 nm over a 6.25 μm^2 region was used as a substrate. Quantitative lateral force measurements require a calibration of the twist elastic constant of the cantilever which can be accomplished by scanning a flat section of surface inclined at a known angle. This calibration method, described by Ogletree *et al.*,[30] was used at room temperature on a facet of a microcrystalline diamond sample.

The DLC surface yielded a normal force curve with a sharp well defined snap to contact, as shown in Fig. 2(a). Friction measurements were taken by applying a symmetric triangular waveform to the x modulation of the RHK control electronics while simultaneously applying a slow ramp to the z piezo as described by Grierson *et al.*[31] The frictional forces on the cantilever act in a direction opposite to the x velocity, which periodically alternates direction. The peak velocity in the x direction was approximately 100 nm/sec. A typical data set is shown in Fig. 2(b) with the twist deflection as a function of the z displacement, which in turn is proportional to the normal force. For a given value of the normal force, the cantilever has two well defined values of the twist corresponding to positive and negative x velocity with a few transient values as the velocity and the twist change sign. The envelope of points forms a horizontal vee emanating from the point of contact. The points which cluster around the arms of the vee represent the upper and lower bands of a conventional lateral force hysteresis loop. Data collected while both approaching and withdrawing from the sample demonstrated repeatability of measurements. The advantage

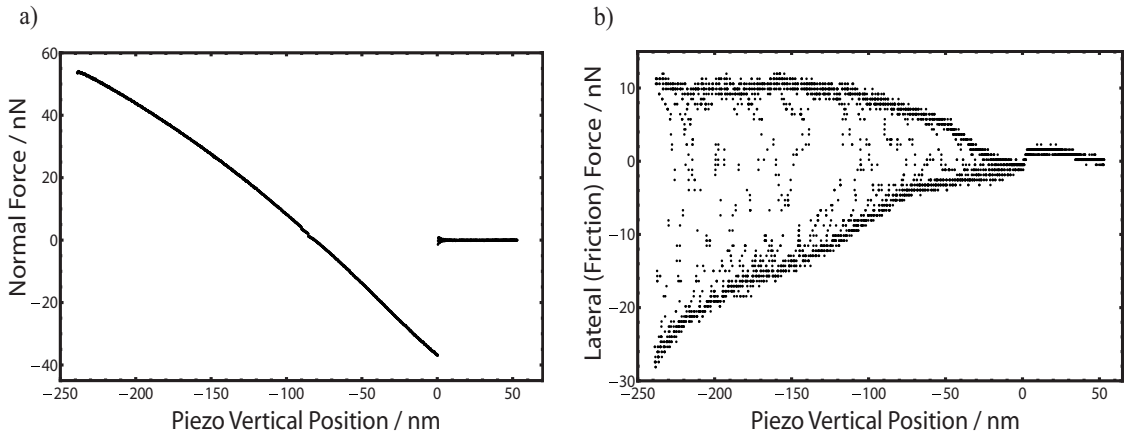

FIG. 2. Normal and lateral force graphs taken at $T=130$ K as a function of the vertical position of the scan head. The zero on the horizontal axis has been adjusted to correspond with the position at which snap down occurs. (a)The normal force increases approximately linearly after snap down with slight deviations likely resulting from piezo nonlinearities, material compression, and nonlinear response of cantilever bending. (b) At the point of contact a friction envelope opens and expands as the normal force increases. The arms of the envelope define two values of lateral force relating to the positive and negative velocities of the tip with a few values inside the envelope due to transients in the tip motion. The asymmetry of the envelope is likely caused by a slope of the sample surface in the direction of horizontal motion.

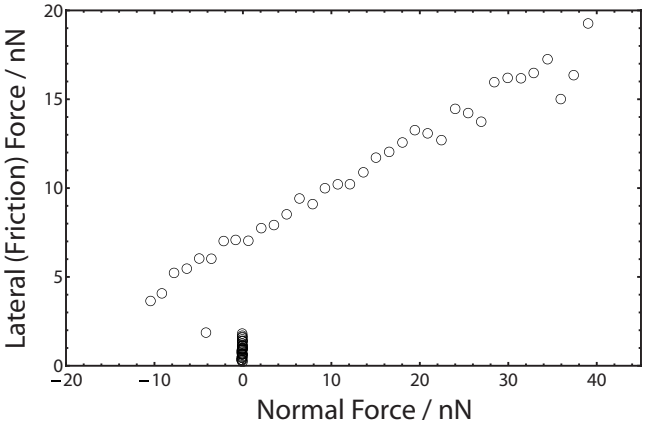

FIG. 3. Lateral (friction) force versus normal force data at a substrate temperature $T=140$ K. For negative values of the normal force, the lateral force is a multivalued function of the normal force due to the nonlinearities of the contact mechanics.

of this technique, as opposed to holding a constant normal force, is that a full range of normal forces can be accessed in a single scan.

The amplitude of the resulting friction envelope is obtained by computing the average of the absolute value of the two lateral force values corresponding to each normal force measurement. A plot of the lateral force as a function of the normal force is shown in Fig. 3. For small values of the normal force near the snap to contact regime, the relationship between the normal and lateral force is nonlinear and multivalued. For normal forces on the upper branch in good contact, the lateral force becomes approximately linear in relation to the normal force. Figure 4 shows the linear part of these force curves for a number of different temperatures ranging from 90–275 K. The slope of the linear fits of the data, taken well after snap down during an approach and well before the pull-off during a withdrawal, provide coefficients of friction that are useful in comparing the friction at various temperatures. The resulting slopes, μ, are shown in Fig. 5.

III. DISCUSSION AND CONCLUSION

Our results show a frictional force which is comparatively independent of the substrate temperature over the

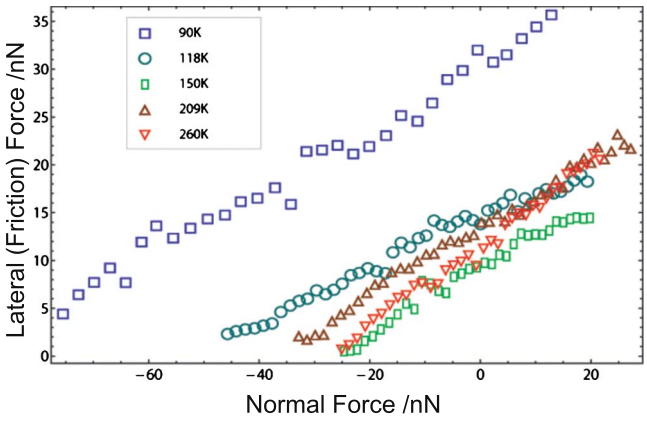

FIG. 4. (Color online) Lateral (friction) force versus normal force data taken at several values of the substrate temperature. The slope of the curves, which corresponds to the coefficient of friction, shows little change with temperature. The work of adhesion, which is proportional to the minimum normal force (Ref. 31) does not seem to vary with temperature until the lowest values of T are reached; similar phenomena have been observed in Ref. 22.

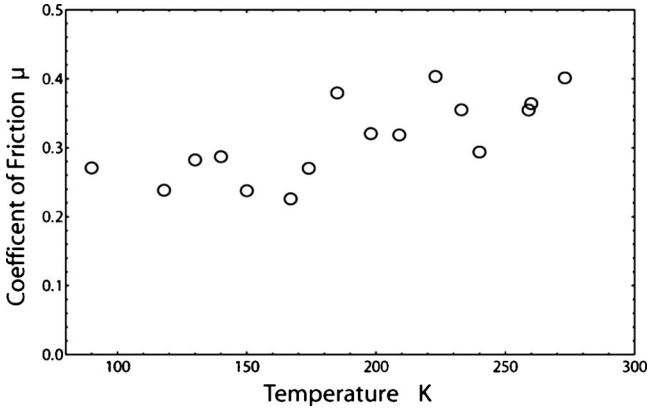

FIG. 5. Slopes taken from linear fits to the curves in Fig. 4 provide coefficients of friction that allow comparison across the range of temperatures sampled. Only a slight linear dependence on the temperature is observed as the friction increases with increasing temperature.

range 90–275 K. This is in marked contrast to some previous studies[15,22–24] on other materials which observed thermally activated behavior and variations of frictional forces by more than an order of magnitude over a similar temperature range. The residual variation in μ of approximately 20% is a monotonically increasing function of temperature. Our results are somewhat similar to those of Brukman *et al.*,[25] who used diamond-coated tips on a single crystal diamond sample and found only a mild dependence of friction over the temperature range of 48 to 225 K. The values of the friction coefficient we observe at room temperature, $\mu \cong 0.4$, are in reasonable agreement with previous AFM measurements on DLC coated silicon,[3] but are considerably higher than macroscopic measurements,[32] which show a slight increase in friction as the temperature is lowered.[29]

Although it might be possible to reconcile these various results by fitting parameters to a thermal hopping model as described in Refs. 13 and 17, to the phonon friction model of Ref. 19, or to the recent model of Barel *et al.*[15] this type of analysis may not be meaningful because it is based on the assumption that the sliding asperity and the substrate are near thermal equilibrium and can be described by a single temperature. Simple thermal modeling as well as direct measurements show that the temperatures can differ by more than 150 K. Variable temperature AFMs which cool the substrate via a connection to a cold finger are designed to thermally isolate the cantilever and the scan head to minimize temperature variations of the piezos which would cause imaging abberations and alignment issues. Even when the substrate is near 100 K, direct measurements of the temperature of the scan tube show that it remains near room temperature.[33] Measurements of the resonant frequency of the cantilever as a function of substrate temperature provide a method of measuring the local temperature of the cantilever independent of its mechanical supports. These measurements also show that the cantilever is always near room temperature and that the temperature remains high even when the tip is brought into contact with the cold substrate.[34] Similar results are obtained when tips equipped with submicron thermocouples are brought into tunneling contact with a cold substrate.[35] The extremely poor thermal contact between a hot tip and a cold

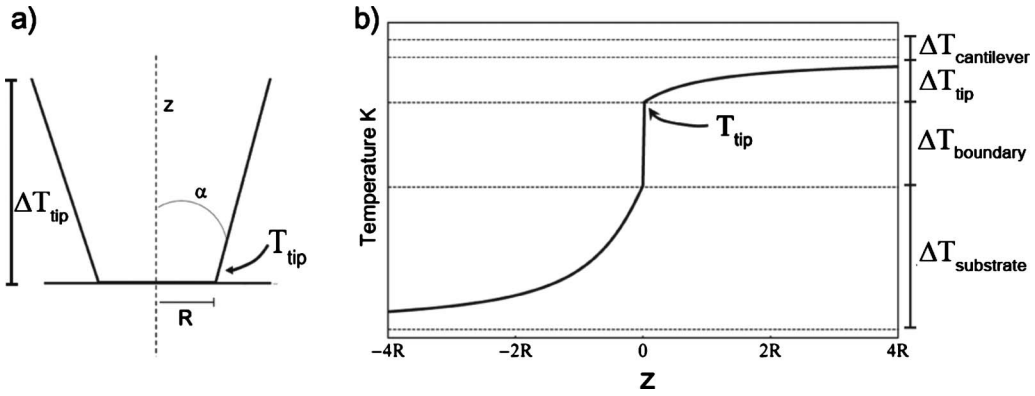

FIG. 6. (a) Schematic diagram of an AFM tip modeled as a truncated cone with half angle α in contact with a substrate in a disk of radius R. (b)Temperature as a function of z near the contact between the tip and substrate at $z=0$. The temperature has a discontinuity at the interface of magnitude T_{boundary}, and large temperature gradients on both sides of the interface which extend within a few units of the characteristic length, R, the radius of the contact. The measured sample temperature $T_{\text{substrate}}$ differs from the temperature T_{tip} by $\Delta T_{\text{substrate}}+\Delta T_{\text{boundary}}$.

substrate in vacuum is distinctly different from the same geometry in air. There is an extensive literature on thermal writing technology[36] which relies on heat transport from a tip through air to the substrate, but when the air is removed the heat transport drops by more than two orders of magnitude.[37]

In vacuum, heat can be transported only by radiation and conduction through solids. A simple calculation shows that radiation is negligible.[33] To analyze the conduction process, it is useful to divide the total temperature drop ΔT from the scan head at temperature $T_{\text{scan head}}$ to the thermometer on the substrate $T_{\text{substrate}}$ into physically distinct pieces. $\Delta T_{\text{cantilever}}$ is the temperature drop along the length of the cantilever. The tip of the cantilever can be regarded as a truncated cone with half angle α in contact with the substrate with a disk of radius R. ΔT_{tip} is the temperature drop from the end of the cantilever to the contact point with the substrate across the truncated cone. The interface between the tip and the substrate produces a thermal impedance which is characterized by a Kapitza resistance,[38,39] or its inverse, a boundary conductance σ. The thermal impedance is due to phonon scattering at the interface and gives rise to a temperature discontinuity at the boundary of magnitude $\Delta T_{\text{boundary}}$. Molecular dynamics calculations verify that the discontinuity is atomically sharp.[40] This temperature discontinuity is proportional to the heat flux and exists at any junction carrying a thermal current, but it is usually negligibly small, so that the temperature can often be regarded as continuous. In the case of a highly localized thermal junction, however, the heat flux can become extraordinarily high generating an unusually large temperature jump at the interface. The finite thermal conductivity of the substrate, $\kappa_{\text{substrate}}$, implies that there is a temperature drop $\Delta T_{\text{substrate}}$ from the contact point to a distant point in the substrate where a macroscopic thermometer is used to measure the substrate temperature $T_{\text{substrate}}$. The various temperatures are related by

$$\Delta T = T_{\text{scan head}} - T_{\text{substrate}} = \Delta T_{\text{cantilever}} + \Delta T_{\text{tip}} + \Delta T_{\text{boundary}} + \Delta T_{\text{substrate}},$$

$$T_{\text{tip}} = T_{\text{substrate}} + \Delta T_{\text{substrate}} + \Delta T_{\text{boundary}}. \quad (1)$$

Each temperature drop drives a thermal current q with units of watts. If the cantilever has a simple geometry with a cross sectional area A and a length L of a material with a thermal conductivity $\kappa_{\text{cantilever}}$, the thermal current would be $q_{\text{cantilever}}=\kappa_{\text{cantilever}}A\Delta T_{\text{cantilever}}/L$, but cantilevers often have complicated geometry and may include several materials, so we describe the heat flow by the relation $q_{\text{cantilever}}=\gamma\Delta T_{\text{cantilever}}$. The temperature inside the tip obeys Laplace's equation with a zero flux condition on the side walls. The solution which satisfies the appropriate boundary conditions is $T(r)=T_{\text{scan head}}-\Delta T_{\text{cantilever}}-R/r\Delta T_{\text{tip}}\csc(\alpha)$, where r is a spherical polar coordinate with origin at the apex of the cone and κ_{tip} is the thermal conductivity of the tip material. The heat current associated with this temperature distribution is $q_{\text{tip}}=\beta\kappa_{\text{tip}}R\Delta T_{\text{tip}}$ where $\beta=4\alpha\csc(\alpha)$ is a geometrical factor. The thermal current across the tip-substrate boundary is proportional to the magnitude of the temperature discontinuity $\Delta T_{\text{boundary}}$, the boundary conductance σ, and the area of contact. The temperature distribution in a half-space with $T=0$ at ∞ due to a uniform heat current distributed over a disk of radius R on the surface is a standard problem of mathematical physics; its solution[41] is

$$T(\rho,z) = \frac{q_{\text{substrate}}}{\pi R\kappa_{\text{substrate}}}\int_0^\infty e^{-\lambda z}J_0(\lambda\rho)J_1(\lambda R)d\lambda, \quad (2)$$

where ρ and z are cylindrical coordinates with the origin at the center of the disk. The average temperature over the disk is simply related to the heat current $q_{\text{substrate}}$ and the thermal conductivity of the substrate $\kappa_{\text{substrate}}$, with $\Delta T_{\text{substrate}}=\frac{8q_{\text{substrate}}}{3\pi^2R\kappa_{\text{substrate}}}$. The temperature on the z axis is given by $T(z)=q_{\text{substrate}}(-z+\sqrt{R^2+z^2})/(\pi R^2\kappa_{\text{substrate}})$. The heat current through the cantilever, tip, boundary and sample are given by:

TABLE I. Temperature values for various tip-substrate combinations. Results of applying Eqs. (1) and (3) to the dimaond/DLC system investigated in this paper and other systems used previously (Refs. 22–25). The thermal boundary conductance was taken to be 10^8 W/Km^2 and $T_{substrate}=100$ K, $\Delta T=170$ K in all cases. The tip temperature, T_{tip}, is greater than $T_{substrate}$ by more than 100 K in every case. The thermal conductivities for diamond, DLC, silicon, silicon nitride, and molybdenum disulphide were taken from Refs. 42–46, respectively. (All units are in S.I.)

Tip	κ	Substrate	κ	γ	$\Delta T_{cantilever}$	ΔT_{tip}	$\Delta T_{boundary}$	ΔT_{sample}	T_{tip}
Diamond	500	DLC	1	1×10^{-4}	≈0	0.2	63	106.8	269.8
Diamond	500	Diamond	500	1×10^{-4}	≈0	0.5	169	0.5	269.5
Silicon	30	Silicon	30	6×10^{-6}	3	8	150.5	8.5	259
Si_3N_4	3	MoS_2	1	6×10^{-7}	10.5	25.5	49.5	84.5	234
Si_3N_4	3	HOPG	3	6×10^{-7}	15.5	38	74.5	42	216.5

$$q_{cantilever}=\gamma\Delta T_{cantilever},\quad q_{tip}=\beta\kappa_{tip}R\Delta T_{tip},$$

$$q_{boundary}=\pi R^2\sigma\Delta T_{boundary}\quad\text{and}\quad q_{substrate}=\frac{3}{8}\pi^2R\kappa_{substrate}\Delta T_{substrate}. \tag{3}$$

In steady state, the heat current through each element must be the same. Setting all the expressions in Eq. (3) equal and solving simultaneously with Eq. (1) yields an expression for the common heat current q in terms of the overall temperature difference ΔT

$$q=\Delta T\left(\frac{1}{\pi\sigma R^2}+\frac{8}{3\pi^2R\kappa_{substrate}}+\frac{1}{\gamma}+\frac{1}{\beta\kappa_{tip}R}\right)^{-1}. \tag{4}$$

Once the heat current q is known, the various temperature differences can be calculated from the expressions in Eq. (3) for any geometry or material parameters. The behavior of the temperature in the vicinity of the contact point is shown in Fig. 6. The only length scale in the problem is the contact radius R, so the temperature in both the conical tip and the substrate approaches their respective far field values at distances of order R.

Table I shows the results of applying Eqs. (1) and (3) for several combinations of cantilever and substrate materials that have been used in variable temperature AFM friction measurements. The calculations have been performed assuming $T_{substrate}=100$ K, $T_{scan\ head}=270$ K, $\Delta T=170$ K, $R=20$ nm, $\alpha=35°$, and $\sigma=10^8$ W/K m^2, which is a typical value for a number of material combinations at room temperature.[38] The table shows that T_{tip} is typically more than 100 K higher than $T_{substrate}$, while $T_{cantilever}$ remains within approximately 15 K of $T_{scan\ head}$, in agreement with experimental results.[34] The heat current through the tip is approximately 10 μW, but the current density is 10^9 W/m^2, which is more than an order of magnitude higher than the heat flux in an arc welder.[47] This high value of the heat flux accounts for the large temperature discontinuities at the boundary. This analysis shows that the tip temperature relatively independent of the substrate temperature. When the thermal conductivity of the substrate is small, the substrate temperature near the contact region is weakly dependent on the measured substrate temperature. In contrast however, the heat flux at the contact point varies by many orders of magnitude (0 to 10^9 W/m^2) over the temperature range of the experiments and is perhaps a more useful parameter to characterize the observed variations in friction.

The picture that emerges from these considerations is that in a conventional variable temperature AFM, the cantilever remains near room temperature and the region near the contact can have extremely high heat fluxes and thermal gradients; the characteristic length scale of the gradients is determined by the contact radius, R. Lateral force data is typically reported as a function of the substrate temperature which can be measured with a macroscopic thermometer, but this temperature can be very different from the temperature in the contact region which presumably affects the microscopic mechanisms of sliding. The total force on the tip is the sum of the friction force and the force due to the cantilever. Since the cantilever is the softest spring in the system with the highest temperature the thermal fluctuations in the cantilever are particularly important and will determine the hopping probability in the models of Refs. 11, 13, and 17. The temperature dependence of single-asperity friction can provide useful insight into mechanisms of friction, and the data reported here along with previous measurements on other materials suggest that a wide variety of behavior is possible. However, a quantitative understanding of these effects and a direct comparison of experiment to theory will require experimental data in which the temperature of the contact is a well defined parameter. A conventional variable temperature AFM, in light of the thermal arguments of this paper, appears to be ill suited to this purpose. Issues caused by temperature gradients and variations in heat flux could be resolved by using an isothermal AFM as described in Refs. 48 and 49 to make the required measurements.

ACKNOWLEDGMENTS

This work has been supported by AFOSR MURI under Grant No. FA9550-04-1-0381.

[1] G. Meyer and N. M. Am, Appl. Phys. Lett. **57**, 2089 (1990).
[2] C. A. J. Putman, V. Igarashi, and R. Kaneko, Appl. Phys. Lett. **66**, 3221 (1995).
[3] C. M. Mate, Wear **168**, 17 (1993).
[4] B. Borovsky, J. Krim, S. A. Syed Asif, and K. J. Wahl, J. Appl. Phys. **90**, 6391 (2001).
[5] B. Dawson, S. M. Lee, and J. Krim, Phys. Rev. Lett. **103**, 205502 (2009).
[6] B. Bhushan, Microelectron. Eng. **84**, 387 (2007).
[7] J. Krim, Am. J. Phys. **70**, 890 (2002).
[8] J. Stiernstedt, H. Brumer, Q. Zhou, T. T. Teeri, and M. W. Rutland, Biomacromolecules **7**, 2147 (2006).
[9] J. Krim, Langmuir **12**, 4564 (1996).
[10] G. A. Tomlinson, Philos. Mag. **7**, 905 (1929).
[11] Y. Sang, M. Dubé, and M. Grant, Phys. Rev. Lett. **87**, 174301 (2001).
[12] E. Gnecco, R. Bennewitz, T. Gyalog, C. Loppacher, M. Bammerlin, E.

Meyer, and H. J. Guntherodt, Phys. Rev. Lett. **84**, 1172 (2000).
[13]S. Y. Krylov and J. W. M. Frenken, J. Phys.: Condens. Matter **20**, 354003 (2008).
[14]I. Szlufarska, M. Chandross, and R. W. Carpick, J. Phys. D: Appl. Phys. **41**, 123001 (2008).
[15]I. Barel and M. Urbakh, Phys. Rev. Lett. **104**, 066104 (2010).
[16]It is important to note, however, that the lateral force is independent of the velocity dependent friction term in the Langevin equation.
[17]Z. Tshiprut, S. Zelner, and M. Urbakh, Phys. Rev. Lett. **102**, 136102 (2009).
[18]B. N. J. Persson, *Sliding Friction: Physical Principles and Applications*, 2nd ed. (Springer, New York, 2000).
[19]V. L. Popov, Tribol. Int. **34**, 277 (2001).
[20]Y. Chen, J. Yang, X. Wang, Z. Ni, and D. Li, Nanotechnology **20**, 035704 (2009).
[21]R. J. Cannara, M. J. Brukman, K. Cimatu, A. V. Sumant, S. Baldelli, and R. W. Carpick, Sciences (N.Y.) **318**, 780 (2007).
[22]X. Y. Zhao, M. Hamilton, W. G. Sawyer, and S. S. Perry, Tribol. Lett. **27**, 113 (2007).
[23]A. Schirmeisen, L. Jansen, H. Holscher, and H. Fuchs, Appl. Phys. Lett. **88**, 123108 (2006).
[24]X. Zhao, S. R. Phillpot, W. G. Sawyer, S. B. Sinnott, and S. S. Perry, Phys. Rev. Lett. **102**, 186102 (2009).
[25]M. J. Brukman, G. T. Gao, R. J. Nemanich, and J. A. Harrison, J. Phys. Chem. C **112**, 9358 (2008).
[26]J. Fontaine, J. L. Loubet, T. L. Mogne, and A. Grill, Tribol. Lett. **17**, 709 (2004).
[27]A. Erdemir and C. Donnet, J. Phys. D: Appl. Phys. **39**, R311 (2006).
[28]R. Hauert, Tribol. Int. **37**, 991 (2004).
[29]M. Aggleton, J. C. Burton, and P. Taborek, J. Appl. Phys. **106**, 013504 (2009).
[30]D. F. Ogletree, R. W. Carpick, and M. Salmeron, Rev. Sci. Instrum. **67**, 3298 (1996).
[31]D. S. Grierson, E. E. Flater, and R. W. Carpick, J. Adhes. Sci. Technol. **19**, 291 (2005).
[32]F. Gao, A. Erdemir, and W. T. Tysoe, Tribol. Lett. **20**, 221 (2005).
[33]Q. Dai, R. Vollmer, R. W. Carpick, D. F. Ogletree, and M. Salmeron, Rev. Sci. Instrum. **66**, 5266 (1995).
[34]D. V. Kazantsev, C. Dal Savio, and H. U. Danzebrink, Rev. Sci. Instrum. **77**, 043704 (2006).
[35]U. F. Wischnath, J. Welker, M. Munzel, and A. Kittel, Rev. Sci. Instrum. **79**, 073708 (2008).
[36]W. P. King, T. W. Kenny, K. E. Goodson, G. Cross, M. Despont, U. Durig, H. Rothuizen, G. K. Binnig, and P. Vettiger, Appl. Phys. Lett. **78**, 1300 (2001).
[37]A. Majumdar, J. Lai, M. Chandrachood, O. Nakabeppu, Y. Wu, and Z. Shi, Rev. Sci. Instrum. **66**, 3584 (1995).
[38]R. J. Stoner and H. J. Maris, Phys. Rev. B **48**, 16373 (1993).
[39]G. L. Pollack, Rev. Mod. Phys. **41**, 48 (1969).
[40]J. W. Lyver and E. Blaisten-Barojas, J. Phys.: Condens. Matter **21**, 345402 (2009).
[41]H. Carslaw and J. Jaeger, *Conduction of Heat in Solids*, 2nd ed. (Oxford University Press, New York, 1959).
[42]J. E. Graebner, S. Jin, G. W. Kammlott, J. A. Herb, and C. F. Gardinier, Appl. Phys. Lett. **60**, 1576 (1992).
[43]M. Shamsa, W. L. Liu, A. A. Balandin, C. Casiraghi, W. I. Milne, and A. C. Ferrari, Appl. Phys. Lett. **89**, 161921 (2006).
[44]C. J. Glassbrenner and G. A. Slack, Phys. Rev. **134**, A1058 (1964).
[45]R. Sultan, A. D. Avery, G. Stiehl, and B. L. Zink, J. Appl. Phys. **105**, 043501 (2009).
[46]R. C. Mclaren, Master thesis, University of Illinois at Urbana-Champaign, 2009.
[47]C. Wu and J. Gao, Comput. Mater. Sci. **24**, 323 (2002).
[48]A. Radenović, E. Bystrenova, L. Libioulle, M. Taborelli, J. A. DeRose, and G. Dietler, Rev. Sci. Instrum. **74**, 1022 (2003).
[49]E. Nazaretski, K. S. Graham, J. D. Thompson, J. A. Wright, D. V. Pelekhov, P. C. Hammel, and R. Movshovich, Rev. Sci. Instrum. **80**, 083704 (2009).